Evanescently Fed Electromagnetic Band Gap Horn Antennas and Arrays

Irina Khromova, Iñigo Ederra, Jorge Teniente, Ramón Gonzalo, *Member, IEEE*, and Karu P. Esselle, *Senior Member, IEEE*

***Abstract*— The design of a horn antenna based on Electromagnetic Band Gap structures (EBGs) and fed by evanescent fields in the containing periodic structure is presented. Such all-dielectric antennas can form compact arrays and provide a promising solution for millimeter, sub-millimeter and THz devices. An evanescently fed EBG horn antenna design based on a woodpile structure and operating at frequencies around 110 GHz is presented, together with experimental and simulation results for an analogous scaled-up prototype antenna operating in the Ku band. It exhibits a 9% bandwidth and an average level of maximum gain approximately equal to 14.6dBi.**

***Index Terms*—electromagnetic band gap (EBG) antenna, horn antenna, sub-millimeter antenna, electromagnetic band gap (EBG) material, array antenna, terahertz antenna, photonic crystal.**

I. Introduction

Electromagnetic band gap structures (EBGs) [1-6], also known as photonic crystals in optics, have been attracting the attention of scientists and technologists since a couple of decades ago. Although a great amount of research has already been conducted in the field of physics and engineering related to EBGs and EBG-based devices, these structures still offer a lot of opportunities in interesting and topical applications.

EBG technology applied to the microwave and THz engineering opens up the possibility of creating compact and well-matched devices due to the fact that an EBG structure can serve as the embedding medium for all the components of such devices. At the same time, the use of EBG structures allows one to avoid losses in metals, which are especially noticeable at high frequencies where the skin-effect becomes significant or dominant [7], as many EBG-based devices can be made almost entirely out of dielectric materials.

In recent years, EBGs have been widely exploited for the purpose of shaping and improving the radiation characteristics of antennas of different types [8-13]. EBG resonator cavities and defects [2-5, 14] have also been used to create antennas with large directivities and high efficiencies [15-17]. The main advantage of these defect-based antennas is their compactness, and their main limitation is the operating bandwidth. All the above mentioned devices also require metallic components.

EBG antennas with larger bandwidths can be designed using the concept of the "classical" metallic horn antennas, consisting of a hollow pipe tapered to form an aperture. As an example, in [18] the idea of matching the transition from an EBG waveguide to free space is considered.

The first two-dimensional photonic crystal horn antenna (PCHA) was reported in paper [19] and in patent [20]. The first physically realizable 3D EBG horn antennas were presented in [21-23]: in these antennas implemented inside a woodpile slab [24,25] the impedance matching between the feeding EBG waveguide and the free space is achieved by introducing a layer of bent woodpile rods.

EBG horn antennas demonstrate a number of advantages and promising properties, such as large operating bandwidth, possibility of reaching high directivity levels, and low losses at higher frequencies due to the absence of metals (provided the components are carefully matched and the level of fabrication errors is low). However, their performance is limited due to the small dimensions of the aperture in the stacking direction. Since the horns are created in one of the woodpile layers, these dimensions are determined by the thickness of the woodpile bars and lead to a broad beam in the E-Plane.

In this paper, a novel way of simultaneously feeding two EBG horn antennas, via evanescent waves, is reported. The design of the evanescently fed EBG horn antennas and arrays are presented. The concept of evanescent feeding is experimentally confirmed.

The paper is organized as follows. Section II explains how hollow defects in EBG structures can function as horn antennas. In the same Section, the concept of evanescent feeding of such antennas is presented together with the design of a F band woodpile-based horn antenna. Section III presents the results of experimental studies of a Ku band scaled-up prototype of the above mentioned antenna. As shown in Sections II and III, the radiation patterns of the proposed antennas are not symmetrical in the E-plane due to geometrical properties of the woodpile structure. Section IV presents the design of a symmetrical two-element array of evanescently fed EBG horn antennas, which exhibits a

Manuscript received August 25, 2010. This work was supported by the Spanish Ministry of Science and Innovation Project Nos. TEC2009-11995 and CSD2008-00066.

I. Khromova, I. Ederra, J. Teniente and R. Gonzalo are with the Electrical and Electronic Engineering Department, Universidad Pública de Navarra, E31006, Pamplona, Navarra, Spain (phone: +34 948 166039; fax: +34 948 169720; e-mail: irina.khromova@unavarra.es, inigo.ederra@unavarra.es, jorge.teniente@unavarra.es, ramon@unavarra.es).

K.P. Esselle is with the Department of Electronic Engineering, Macquarie University, Sydney, NSW 2109, Australia (e-mail: karu.esselle@mq.edu.au).

symmetrical radiation pattern in both E- and H-planes. Conclusions are presented in Section V.

II. Evanescently fed EBG horn antennas

A. *Horn antennas in a woodpile structure*

In this work, the woodpile structure (Fig.1) is used as the embedding medium due to its relative simplicity in terms of fabrication [26]. For the frequencies around 90-120GHz the chosen EBG structure is assumed to be made of silicon bars with dielectric permittivity and loss tangent equal to ε=11.9 and $tan\delta$=0.004, respectively. The geometrical parameters of the woodpile are: EBG lattice constant a=1mm, width and height of the silicon rods equal to d_1=0.3mm and d_2=0.33mm respectively. According to plane wave decomposition calculations the chosen woodpile structure exhibits a band gap in the frequency range of approximately 95-125GHz.

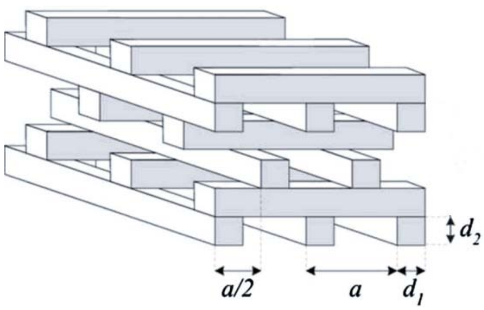

Fig.1. Woodpile structure. Here, a is the lattice constant and d_1 and d_2 are the width and height of the woodpile rods, respectively.

The horn antenna is realized as a hollow pyramidal-shaped defect of the ideal periodic woodpile. Such a defect can be created in one layer of the woodpile structure by bending the rods as shown in Fig.2 (as proposed in [22,23]).

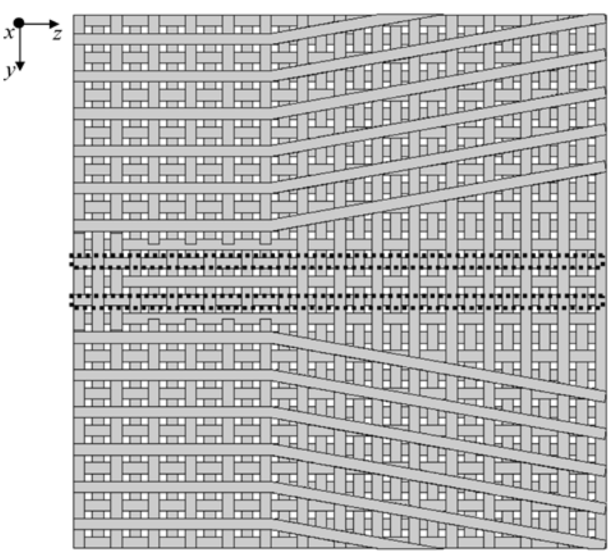

Fig.2. EBG horn antenna made formed by bent woodpile rods and coupled directly to an EBG waveguide. Two woodpile rods, parallel to the waveguiding direction (marked by black dashed lines) were removed in order to create a hollow defect in the periodic structure.

The EBG horn antenna in Fig.2 is directly coupled to a feeding EBG waveguide. This configuration will be used as a reference for directivity analysis below.

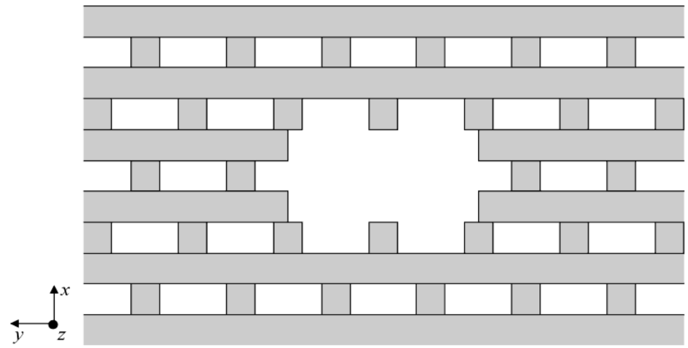

Fig.3. Three-layer woodpile waveguide. Two woodpile rods, parallel to the waveguiding direction, and parts of the rods from the adjacent layers perpendicular to the waveguiding direction, have been removed to form this defect waveguide.

In this paper, a three-layer EBG waveguide (illustrated in Fig.3) is used as a feeding waveguide for the EBG horn antennas. This waveguide, realized as a hollow defect in three adjacent layers of a woodpile structure, is a non-symmetrical scaled version of the one reported in [27] (i.e. there is no mirror symmetry in the stacking direction of the woodpile layers). The latter showed a very good matching with standard WR10 metallic microwave waveguide in the W band (75 – 110 GHz). The EBG waveguide used for the present antenna configuration is formed by removing two woodpile rods parallel to the waveguiding direction and parts of the perpendicular woodpile bars in the adjacent upper and lower layers of the periodic structure. This EBG waveguide operates in the F band at around 100-120GHz. Its numerically calculated transmission and reflection coefficients, when the device is fed by a WR8 waveguide, are shown in Fig.4. The system was simulated using the FDTD method (provided by CST Microwave Studio).

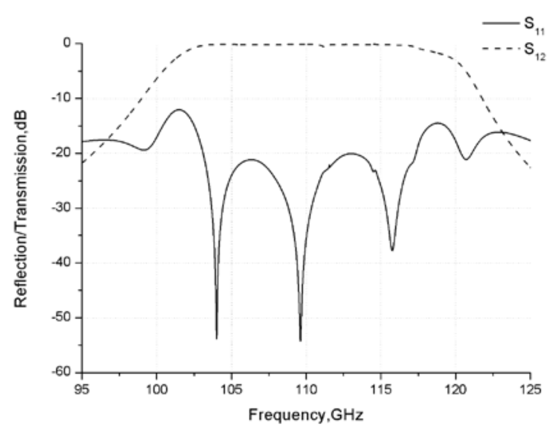

Fig.4. Numerically calculated transmission and reflection of the three-layer woodpile waveguide when fed via WR8 waveguide.

In Fig.5 the input reflection coefficient, directivity and gain of the simulated single-layer EBG horn antenna are presented.

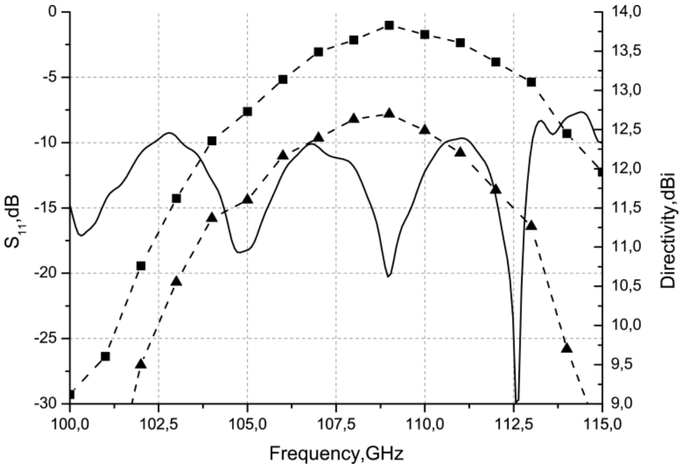

Fig.5. Performance of the single-layer woodpile horn antenna fed by a three-layer woodpile waveguide. The black solid curve represents the antenna input reflection coefficient magnitude. The dashed lines with black squares and triangles represent the peak directivity and gain of the antenna, respectively.

Considering the level of reflection, efficiency and directivity of the simulated device, its operating bandwidth can be estimated as approximately 9%: in the interval of 103.27-113.03GHz the reflection coefficient tends to stay below the value of -10dB, and the directivity does not decrease for more than 3dBi from its maximum value.

A typical radiation pattern of this EBG horn antenna is presented in Fig.6.

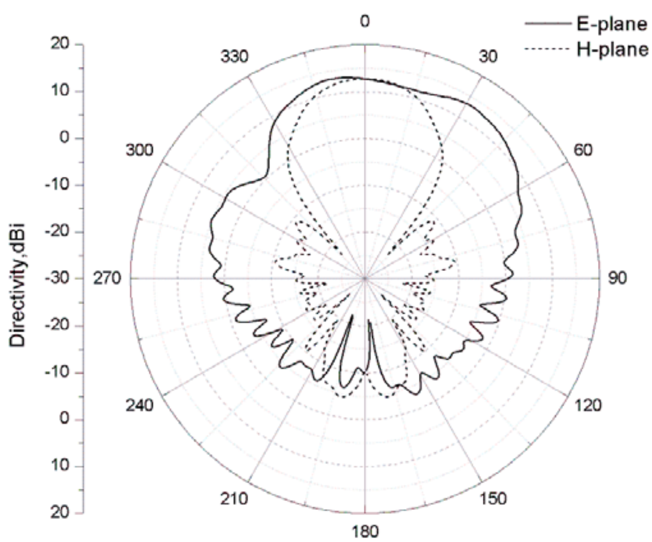

Fig.6. E- and H-plane radiation patterns at 110GHz.

It can be noticed that the main lobe of the radiation pattern is quite wide in the E-plane (the stacking direction of the woodpile). While the width of the lobe in the H-plane can be controlled by changing the antenna flare angle, the main lobe in the E-plane can hardly be made narrower, since the considered antenna is an H-plane sectoral horn antenna formed within one layer of the woodpile structure. This type of EBG structure does not allow bending rods in both planes simultaneously, which can be seen clearly looking at the woodpile structure. This means that a pyramidal horn antenna based on woodpile structure cannot be realized in a straightforward way. An alternative approach lying in constructing pyramidal woodpile horn antennas from separate blocks of woodpile is reported in [28].

The absence of symmetry of the radiation pattern in the E-plane clearly seen in Fig.6 arises also due to the peculiar geometry of the embedding woodpile structure. The problem of the symmetry of EBG horn antennas radiation patterns will be discussed below.

B. EBG horn antennas fed via evanescent fields

In order to reduce the beamwidth in the E-plane an alternative feeding configuration is proposed. Instead of the direct coupling of the horn antenna to the waveguide, the evanescently fed EBG horn antenna (Fig.7) uses the “tunnelling” effect, which occurs in the EBG structures, as a coupling mechanism to transfer the energy from the feeding waveguide to the EBG antenna. This approach makes it possible to use one EBG waveguide to feed two closely placed EBG horn antennas, thus allowing the realization of compact EBG horn antenna arrays [23] and achieving narrower beams in the E-Plane.

In the present paper, an evanescently fed double EBG horn antenna is presented (Fig.7). It consists of two horns such as that previously described, formed by layers of bent rods placed at a distance of two vertical periods of woodpile ($8d_2$) and a common three-layer EBG waveguide feed. This configuration can be also considered as a two-element array, but since both apertures share the feeding EBG waveguide, in this paper it will be referred to as a “double EBG horn antenna”. The distance between the antennas was set to two periods of the woodpile structure simply because smaller separation results in combining both antennas in a single defect lying within the same period of the EBG structure. This would lead to deterioration of the horn antenna performance. The dramatic effect of mutual strong coupling of the closely placed antennas was described in details in [23]. Larger distances do not permit using a common waveguide feed due to losses in the EBG structure, and do not provide the necessary interference between the apertures.

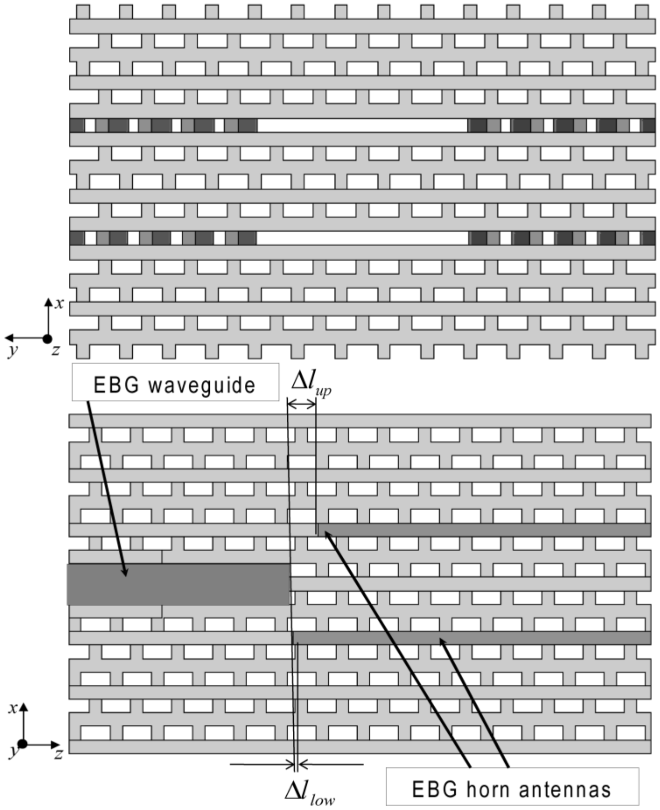

Fig.7. Front- and side-view of the evanescently fed double EBG horn antenna. Dark areas represent the feeding EBG waveguide region and the EBG horn antenna layers. The waveguide and antennas are not connected directly.

Both evanescently fed antennas have the same flare angle α=10º. Fig.8 presents the input reflection coefficient for different flare angles, and it can be seen that α=10º is the optimal flare angle for the considered woodpile parameters in terms of bandwidth and reflection level.

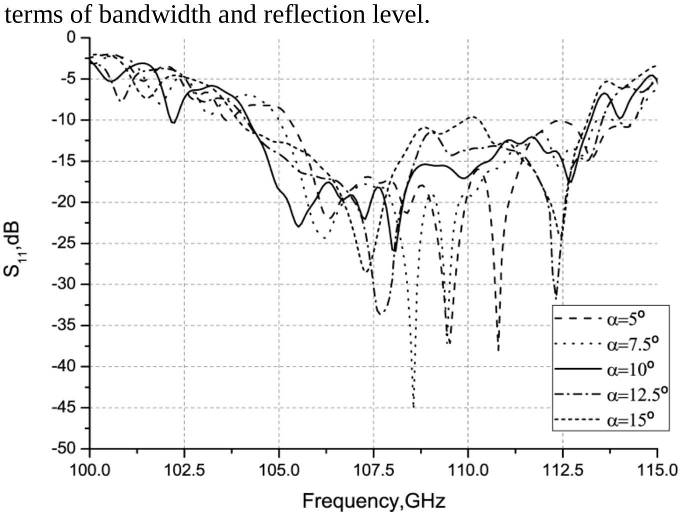

Fig.8. Simulated input reflection coefficient of the evanescently fed double EBG horn antenna at different values of the flare angle α.

The position of the upper antenna throat is shifted with respect to the lower antenna for a half-period of the woodpile (exact value determined by parametric analysis) in order to provide better waveguide-to-antenna coupling due to the intrinsic asymmetry of the EBG woodpile structure in the vertical direction. Thus, the aperture of the lower antenna is insignificantly wider than that of the upper antenna.

In order to define the optimal position of the EBG horn antennas, the reflection coefficient was calculated for the structures where the upper and the lower horns were shifted along the *z*-axis for $\Delta l_{up} \in [0,2a]$ and $\Delta l_{low} \in [0,2a]$, respectively, with reference to the end position of the EBG waveguide. The reflection coefficient calculated at different antenna positions are presented in Fig.9. These are the overview of the computed cases, which demonstrate the range of variation obtained. The optimal positions in terms of input reflection coefficient are $\Delta l_{up}=0.6a$, $\Delta l_{low}=0$.

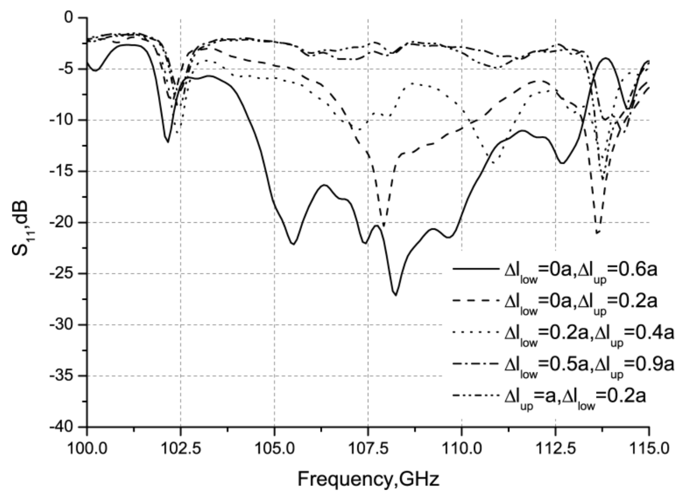

Fig.9. Simulated input reflection coefficient of the evanescently fed double EBG horn antenna at different positions of horns with respect to the feeding waveguide.

Moreover, setting the antenna positions as $\Delta l_{up}=0.6a$, $\Delta l_{low}=0a$ makes both horns radiate in phase for the central frequency ($f \approx 108.7$GHz). Fig. 10 presents the dependence of the phase difference of the electric field in the upper and lower EBG horn antennas $\Delta\varphi$ on the coordinate in the direction of propagation (*z*) for different frequencies. At the edges of the operating band, the phase mismatch increases up to 20º and 10º for the lower and upper frequency band boundary, respectively.

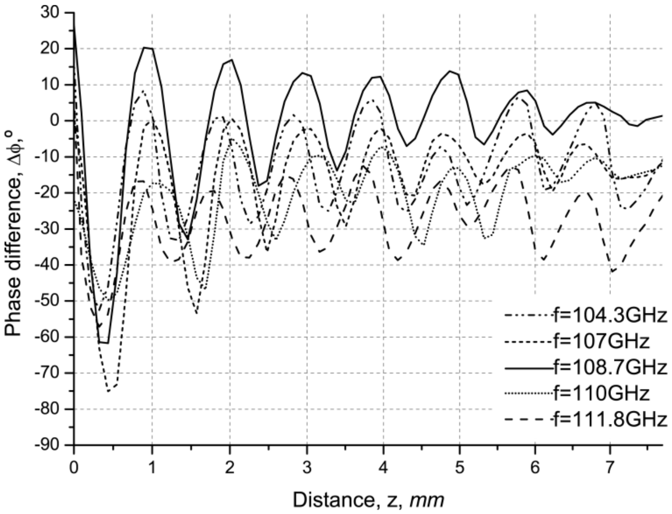

Fig.10. Simulated phase difference of the electric field in the upper and lower EBG horn antennas vs. displacement in the direction of propagation for different frequencies within the operating frequency band. The point z=0 corresponds to the upper antenna throat position.

At the same time, the chosen parameters provide almost equal coupling between the feeding waveguide and each of the horns. Fig.11 presents the corresponding coupling levels, CL_{21} and CL_{31}, equal to S-parameters (S_{21} and S_{31}, respectively) normalized to have a maximum value of unity (or 0dB). The coupling levels were calculated numerically by putting a probe at the apertures of each of the horns for different antenna positions.

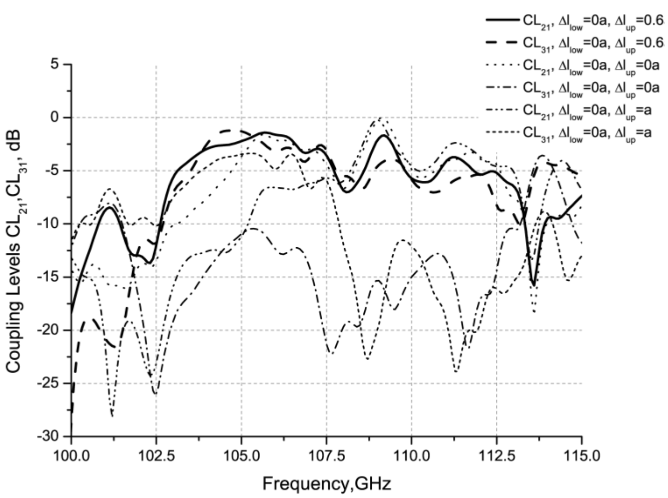

Fig.11. Simulated levels of coupling between the feeding EBG waveguide and the lower and the upper EBG horns (CL_{21} and CL_{31}, respectively) at different positions of horns with respect to the feeding waveguide.

Fig.12 presents the field distribution in different cross-sections of this antenna configuration at 108 GHz. In the woodpile middle layer, where the input waveguide is located, the field is blocked by the woodpile structure. It can be seen that in the upper and lower woodpile horns, the field behaves as it should do in a horn antenna.

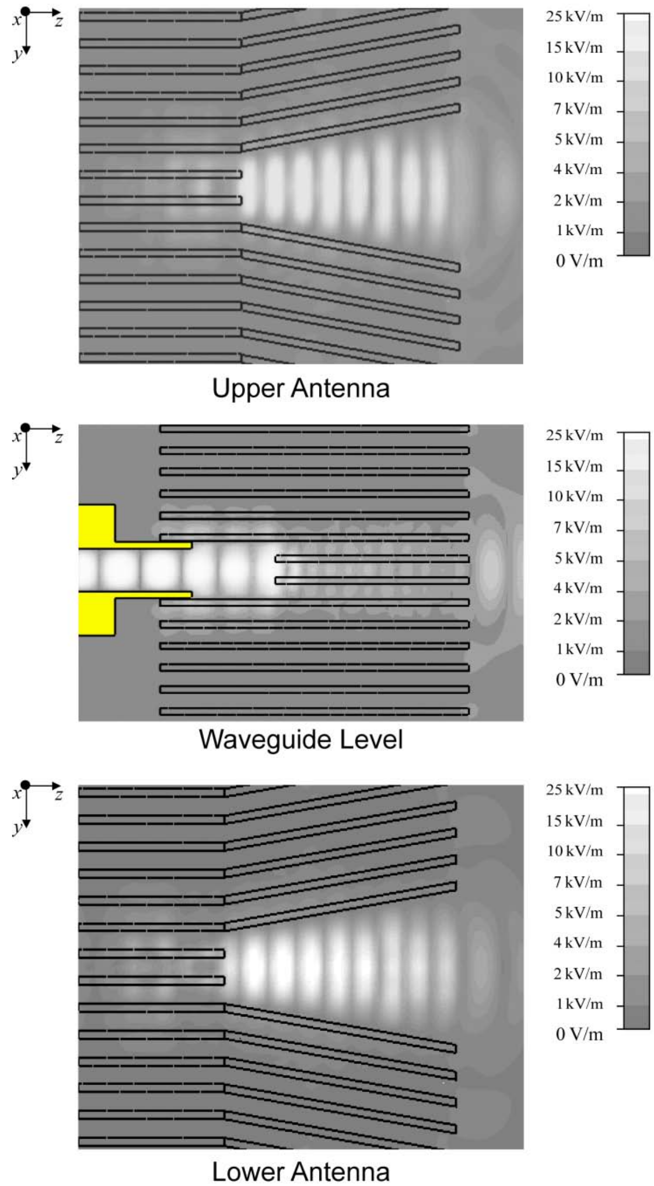

Fig.12. Electric field distribution (absolute value in gray-scale) at 108 GHz in the cross-sections corresponding to the lower antenna plane (H-plane), waveguide middle level plane (H-plane) and upper antenna plane (H-plane).

The reflection coefficient, directivity and gain of the antenna are presented in Fig.13.

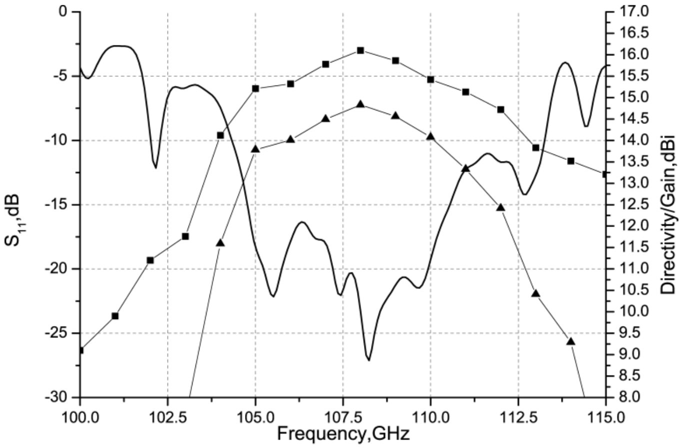

Fig.13. Simulated performance of the evanescently fed EBG horn antenna. The black solid curve represents the antenna input reflection coefficient magnitude. The solid curves with squares and triangles represent the peak directivity and gain of the evanescently fed double EBG horn antenna respectively.

In terms of reflection, efficiency and directivity the device has approximately 8.3% bandwidth: in the interval of 104.20-113.25GHz the reflection coefficient stays below the value of -10dB, the directivity does not decrease for more than 3dBi from its maximum value, and the radiation efficiency is sufficiently higher than -3dB (50%). The maximum value of the gain of the evanescently fed EBG horn antenna (14.9dBi) is more than 2dB higher than that of the previously considered directly-fed EBG horn antenna (Fig.5). The matching of the horn is also improved with respect to the first configuration.

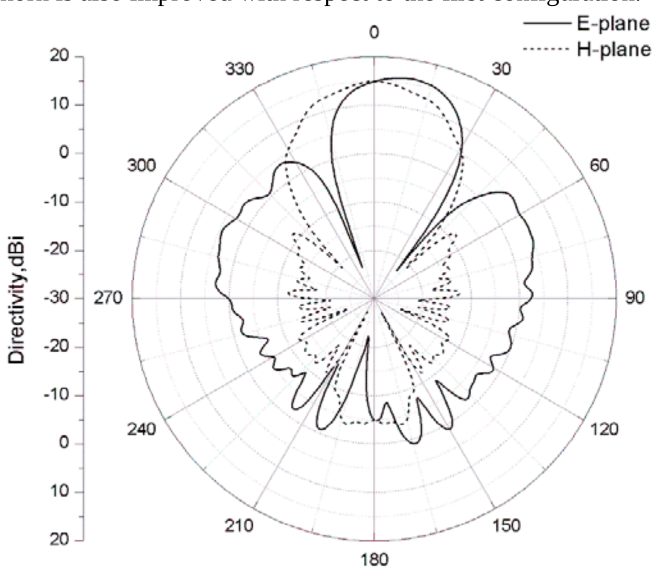

Fig.14. Simulated E-plane and H-plane radiation patterns at 110GHz.

In Fig.14 the E- and H-plane radiation patterns at a selected frequency of 110 GHz are shown. It can be seen that both in Fig.14 and Fig.6 the E-plane radiation pattern is not symmetrical and the main lobe is slightly tilted. This happens due to the phase shift between the array elements and the absence of vertical mirror symmetry in the woodpile structure. The pronounced side lobes in Fig.14 are the grating lobes. However, their level is comparatively reasonable as the difference between the directivity values of the main- and the side-lobes is greater than 10dB within the operating bandwidth.

III. Prototype EBG horn antenna in Ku band

In order to confirm the results of the simulations and to corroborate the concept of evanescent feeding in EBGs, a low-frequency prototype of the above described EBG horn antenna, with scaled-up parameters, was fabricated and measured.

The woodpile structure with the period equal to 8.5mm and having a band gap in the Ku frequency band (at around 12.6-15.7GHz) was fabricated from 1.27mm-thick slabs of Rogers RC3010 (dielectric constant ε =11.2) using a milling machine with a 2mm end mill. The parameters of the woodpile were chosen as follows: EBG lattice constant a = 8.5*mm*, woodpile bars width and height equal to d_1=2.8mm and d_2=2.54mm respectively. The flaring angles of the upper and lower antennas were chosen to be equal to 10º in order to obtain the best matching and radiation properties. Note that the structure is not a directly scaled-up version of the previously presented one, slight adjustments of the geometry of the structure had to be performed due to the limited range of thickness of the used dielectric material and the small variation in the dielectric constant.

The EBG structure was mounted layer by layer (Fig.15) and fixed firmly in order to avoid displacements and distortions affecting the geometrical structure and the periodicity of the woodpile. The evanescently fed double EBG horn antenna was fed by a metallic waveguide introduced into the structure.

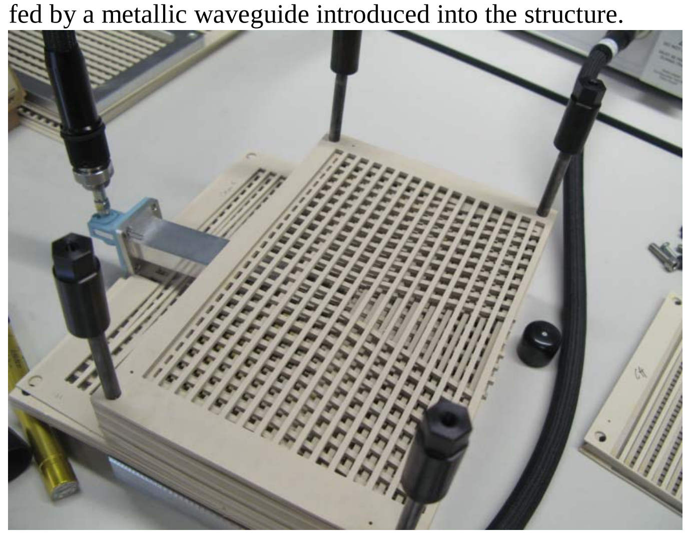

Fig.15. The scaled-up low-frequency prototype of the double evanescently fed EBG horn antenna at the stage of mounting.

With the use of a network analyzer PNA E8361C, the input reflection coefficient S_{11} was measured at the frequencies within the range of 12-18GHz. The results of the reflection measurements, presented in Fig.16, show a very good agreement between the experimental and numerically predicted data. According to the simulations, the antenna exhibits approximately a 10.1% bandwidth and operates in the frequency range of 13.17 – 14.57GHz. The measurements confirm a slightly narrower 9.05% bandwidth, which corresponds to the 13.3 – 14.56GHz frequency range.

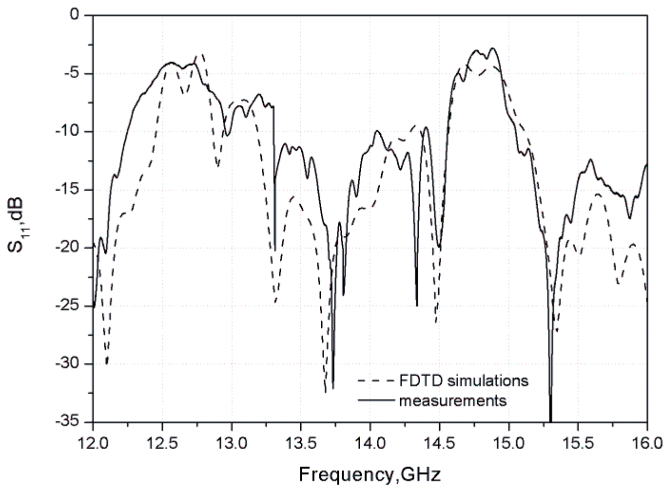

Fig.16. Simulated and measured input reflection coefficient of the Ku band prototype of the double evanescently fed EBG horn antenna.

The simulated and measured antenna maximum gain is presented in Fig.17. The peak value is equal to 14.6dBi.

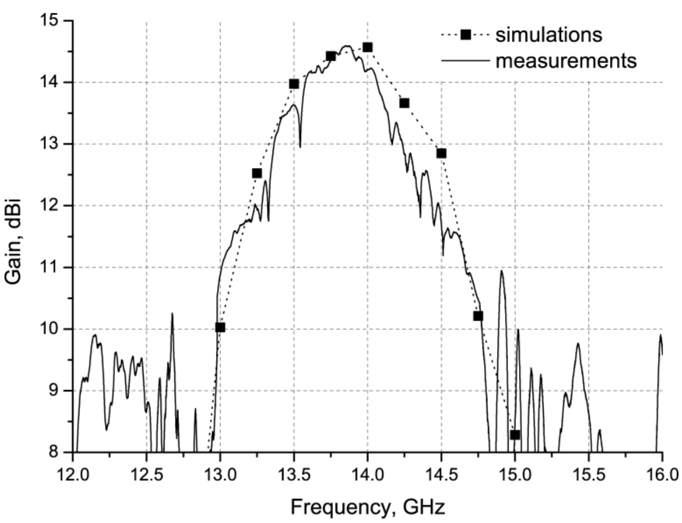

Fig.17. Simulated and measured peak gain of the Ku band prototype of the double evanescently fed EBG horn antenna.

Fig.18 and Fig.19 present the experimentally obtained radiation patterns and the corresponding FDTD simulation data for three different frequencies within the band gap. A good agreement between simulation and experimental data was achieved again.

A slight asymmetry of the radiation pattern in the E-plane of the antenna can be noticed. This phenomenon occurs due to the absence of vertical symmetry in the woodpile structure, as it was previously explained.

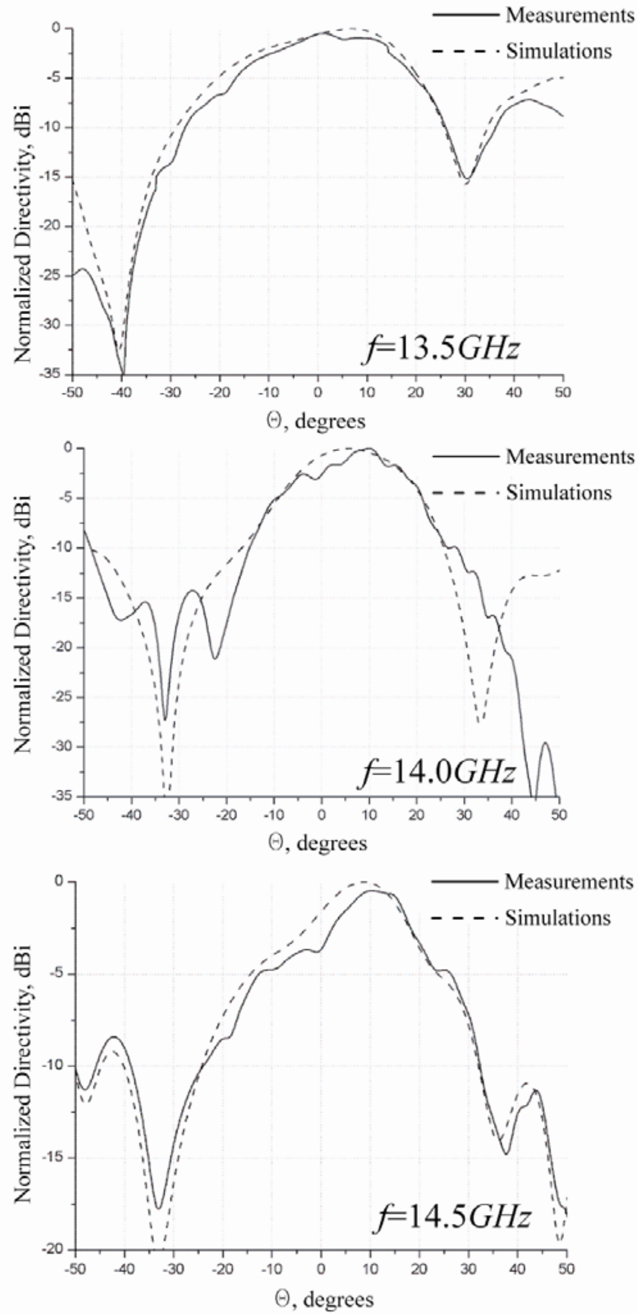

Fig.18. Simulated and measured E-plane radiation patterns of the Ku band prototype of the double evanescently fed EBG horn antenna at 13.5GHz, 14.0GHz and 14.5GHz.

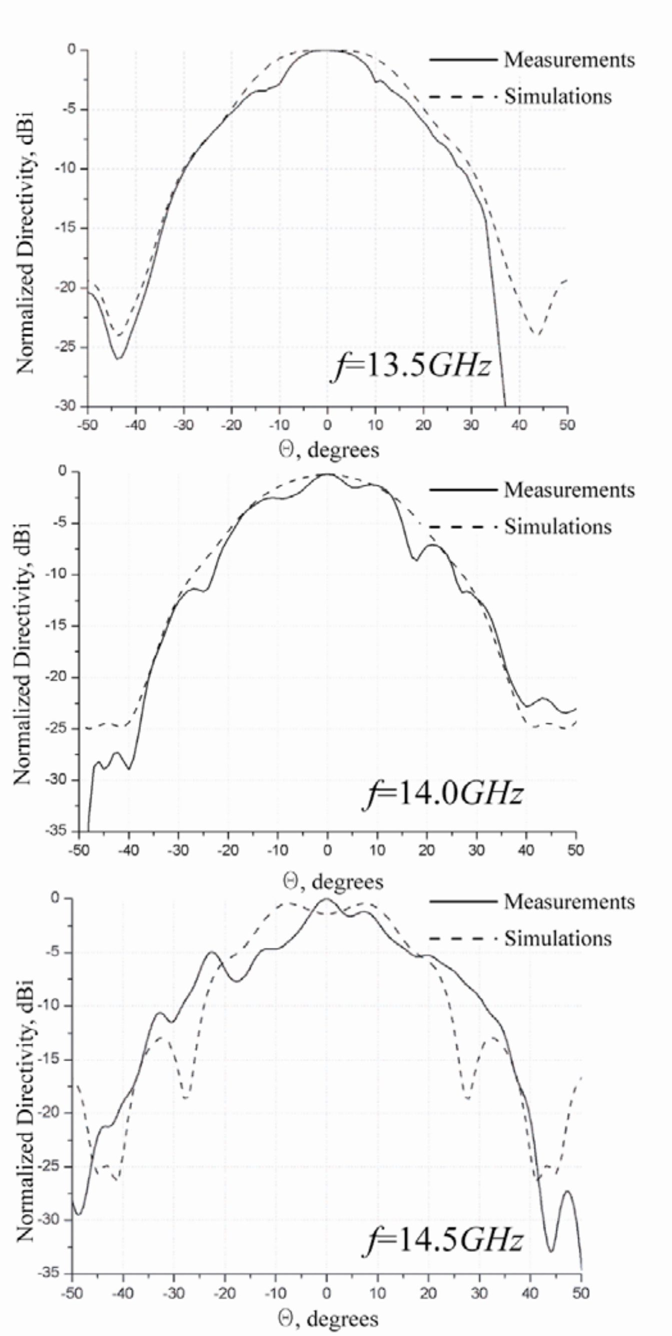

Fig.19. Simulated and measured H-plane radiation patterns of the Ku band prototype of the double evanescently fed EBG horn antenna at 13.5GHz, 14.0GHz and 14.5GHz.

IV. Symmetrical array of evanescently fed EBG horn antennas

In the previous section, the principle of evanescent feeding was demonstrated experimentally. This approach can be used in order to create compact arrays of EBG horn antennas [23] since more than one antenna can be fed by one EBG waveguide, and the problem of having to leave considerable distance between the latter ones is automatically solved. At the same time, less input/output ports are required.

However, as it has already been mentioned, since woodpile structures possess no mirror symmetry in the vertical (stacking) direction, the main lobe of the radiation pattern of a woodpile horn antenna will always point slightly upwards or downwards. In order to sort this problem out and obtain a symmetrical radiation pattern in both E- and H-planes, a symmetrical array of two evanescently fed double EBG horn antennas (four EBG horns fed by two EBG waveguides) was designed (Fig. 20).

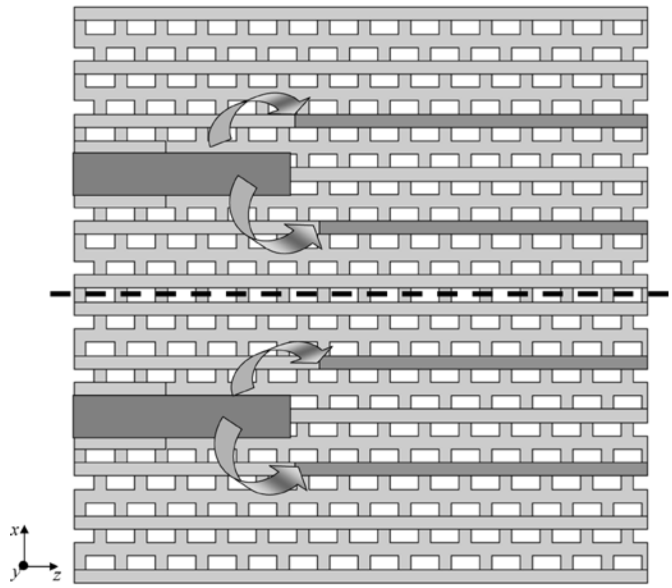

Fig.20. Symmetrical array of four EBG horn antennas evanescently fed by two EBG waveguides. The mirror symmetry plane is marked by the dashed line. Dark areas represent the feeding EBG waveguide region and the EBG horn antenna layers. The arrows show the direction of energy coupling.

In this structure, a mirror symmetry layer is introduced in the woodpile structure. A symmetry layer in an EBG, being a defect of the periodic structure, may affect the band gap properties. However, in the present configuration there is enough space between the horns and waveguides and this “defect layer” for the band gap to become apparent. In other words, the introduced vertical symmetry does not affect the functioning of the EBG-based components of the presented antenna.

Vertical symmetry results in such an interaction of the radiating apertures that the resulting main lobe points to boresight and the radiation pattern becomes symmetrical in both E- and H-planes (Fig.21).

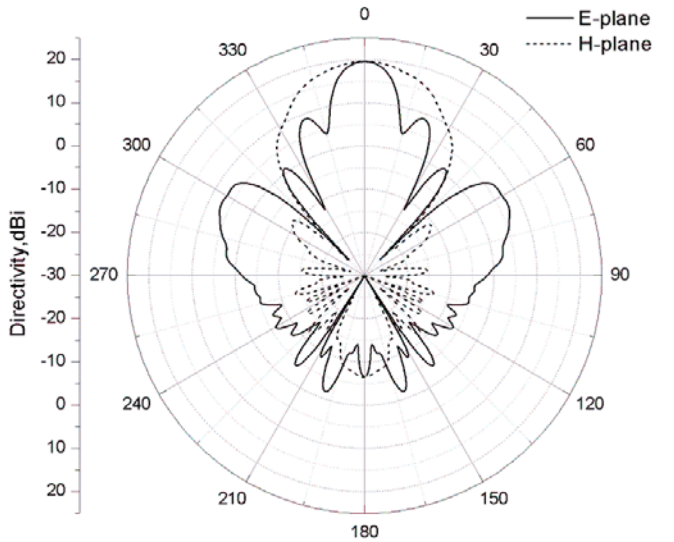

Fig.21. Simulated E- and H-plane radiation patterns of the symmetrical array at 110GHz.

It can be clearly seen that the radiation pattern becomes symmetric. The maximum directivity at 110GHz is 19.6dBi, being increased by almost 4dBi compared to the double EBG horn antenna configuration. The side lobes are still present. However, the difference between the main and the side lobe level is greater than 10dB.

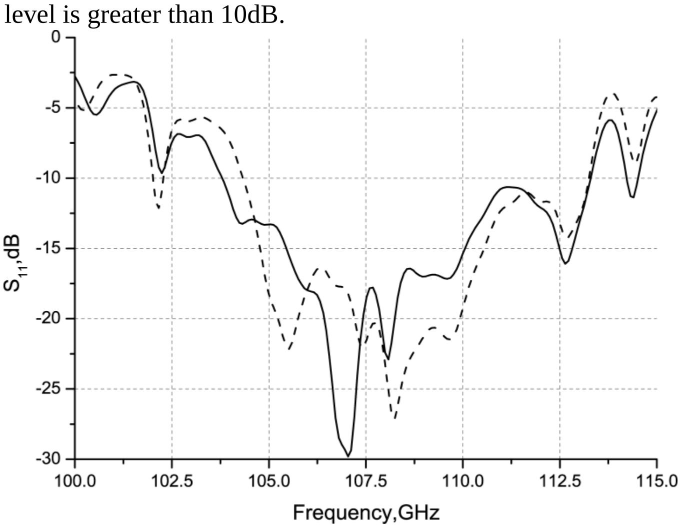

Fig.22 Simulated input reflection coefficients of the symmetrical EBG horn antenna array (solid curve) and the double EBG horn antenna sub-array (dashed curve).

The level of input reflection of the symmetrical array presented in Fig. 22 is similar to the level of reflection of the array components, i.e. the double evanescently fed EBG horn antennas (Fig.13). Thus, the operating bandwidth of the two presented configurations is practically the same.

The spatial distribution of the electric field in the symmetrical EBG horn antenna array at 110GHz is presented in Fig.23.

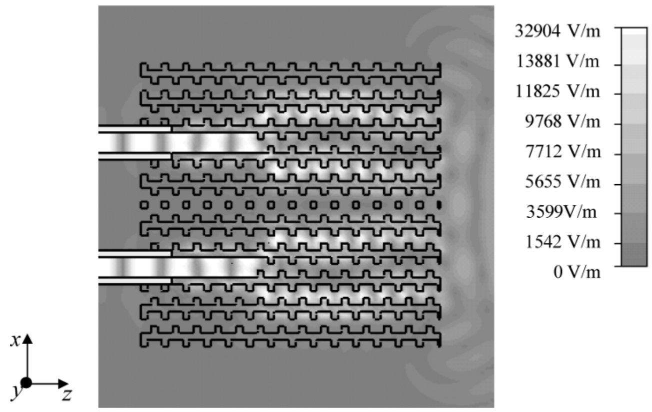

Fig.23. Electric field distribution (absolute value in grey-scale) at 110GHz in the E-plane cross-section of the array of four evanescently fed EBG horn antennas.

Thus, the designed symmetrical array of four woodpile horn antennas allows one to obtain all the advantages of the evanescently fed EBG horn antennas and at the same time to achieve symmetry in the radiation pattern.

V. Conclusion

In this paper, the concept of evanescent feeding of EBG horn antennas is presented. It has been developed and confirmed numerically and experimentally. The proposed type of antennas is interesting and promising from the practical point of view as they can be easily stacked together to form an array within the same EBG slab. Thanks to evanescent feeding, fewer input/output ports are required.

A double evanescently fed EBG horn antenna for millimeter wavelengths has been designed and simulated. It exhibits a 8.3% bandwidth and an average level of maximum directivity approximately equal to 16dBi. A prototype of this device in Ku frequency band has been fabricated and measured. The experimental results show good agreement with simulations and confirm the efficiency of the concept of evanescent feeding for EBG horn antennas.

A solution for the problem of asymmetrical radiation patterns of woodpile horn antennas has been presented. Using a mirror-symmetry layer between two double EBG horn antennas, one can realize a four-antenna array fed evanescently by two EBG waveguides. Such an array possesses a symmetrical radiation pattern and a considerable operating bandwidth: more than 8% for the presented F band design.

References

[1] E. Yablonovitch, “Inhibited spontaneous emission in solid-state physics and electronics”, *Phys. Rev. Lett*, vol. 58, pp. 2059-2062, 1987.

[2] S. John, "Strong Localization of Photons in Certain Disordered Dielectric Superlattices", *Phys. Rev. Lett,* vol. 58, p.2486, 1987.

[3] R. D. Meade, K. D. Brommer, A. M. Rappe, and J. D. Joannopoulos, “Photonic bound states in periodic dielectric materials”, Phys Rev B, vol. 44 (24), pp. 13772-13774 (1991).

[4] J. D. Joannopoulos, R. D. Meade, J. N Winn, *Photonic crystals*, Princeton University Press, 1995.

[5] J. D. Joannopoulos, P. R. Villeneuve, and S. Fan, “Photonic crystals: putting a new twist on light”, *Nature*, vol. 386, p. 143, 1997.

[6] K. M. Ho, C. T. Chan, and C. M.,Soukoulis, "Existence of a photonic gap in periodic dielectric structures", *Phys. Rev. Lett*., vol. 65, p.3152, 1990.

[7] P. Waldow, I. Wolff, "The Skin-Effect at High Frequencies", *IEEE Trans. on Microwave Theory and Techniques*, vol. MTT-33, no. 10, pp. 1076-1082, 1985.

[8] E.R. Brown, C.D. Parker, E. Yablonovitch, "Radiation properties of a planar antenna on a photonic-crystal substrate", *J. Opt. Soc. Am. B*, vol. 10 (2), pp.404-407, 1993.

[9] R. Gonzalo, I. Ederra, C.M. Mann and P. de Maagt, "Radiation Properties of Terahertz Dipole Antenna mounted on Photonic Crystal", Electronics Letters, vol. 37, no. 10, pp. 613-614, May 2001.

[10] I. Ederra, R. Gonzalo, B.E. J. Alderman, P.G. Huggard, B.P. de Hon, M.C. van Beurden, A. Murk, L. Marchand, P. Maagt, "Electromagnetic BandGap based Planar Imaging Array for 500 GHz", *IEEE Trans. on Microwave Theory and Techniques*, vol. 56, no. 11, pp. 2556-2565, Nov. 2008.

[11] M. P. Kesler, J. 0. Maloney, B. L. Shirley, "Antenna design with the use of photonic band-gap materials as all-dielectric planar reflectors", *Microwave and Optical Technology Letters*, vol. 11(4), pp.169-174, 1996.

[12] G.S. Smith, M.P. Kesler, and J.G. Maloney, "Dipole antennas used with all-dielectric, woodpile photonic-bandgap reflectors: gain, field patterns, and input impedance", *Microwave Opt. Technol. Lett*., vol. 21(3), pp. 191-196, 1999.

[13] Z. Zhao, Q. Deng, H. Xu, Ch. Du, X. Luo "A sectoral horn antenna based on the electromagnetic band-gap structures", *Microwave and Optical Technology Letters*, vol. 50(4), pp. 965-969, 2008.

[14] I.Khromova, R.Gonzalo, I.Ederra and P.de Maagt, "Resonance frequencies of cavities in three-dimensional electromagnetic band gap structures", *Journal of Appl. Phys*., vol. 106 (1), pp. 014901.1-7, 2009.

[15] C. Serier, C. Cheype, R. Chantalat, M. Thevenot, T. Monediere, A. Reinex, and B. Jecko, "1-D photonic bandgap resonator antenna", *Microwave Opt. Technol. Lett*., vol. 29(5), pp.312-315 (2001)

[16] C. Cheype, C. Serier, M. Thevenot, T. Monediere, A. Reinex, and B. Jecko, "An electromagnetic bandgap resonator antenna", *IEEE Trans. Antennas Propag*. vol. 50(9), pp. 1285-1290, 2002.

[17] R. Biswas, E. Ozbay, B. Temelkuran, M. Bayindir, M.M. Sigalas, and K.M. Ho, "Exceptionally directional sources with photonic-bandgap crystals", *J. Opt. Soc. Am. B*, vol. 11, pp. 1684-189, 2001.

[18] E. Moreno, D. Erni, and C. Hafner, "Modeling of discontinuities in photonic crystal waveguides with the multiple multipole method", *Phys. Rev. E*, vol. 66(3), pp. 036618-036630, 2002.

[19] A. R. Weily, K. P. Esselle, B. C. Sanders, "Photonic crystal horn and array antennas", *Phys. Rev. E* vol. 68, pp. 016609-1-016609-6, 2003.

[20] R. L. Moore, M. P. Kesler, J. G. Maloney, and B. L. Shirley, US Patent 5,689,275, 1997.

[21] A. R. Weily, K. P. Esselle, B. C. Sanders , T.S. Bird, "High-gain 1d ebg resonator antenna", *Microwave and Optical Technology Letters*, vol. 47(2), pp.107-114, 2005.

[22] A. R. Weily, K. P. Esselle, B. C. Sanders, "Layer-by-layer photonic crystal horn antenna", *Phys. Rev. E*., vol. 70, pp. 037602-4, 2004.

[23] A. R. Weily, K. P. Esselle, T.S. Bird, B. C. Sanders "Linear Array of Woodpile EBG Sectoral Horn Antennas", *IEEE Transactions on Antennas and Propagation*, vol. 54(8), pp. 2263-2274, 2006.

[24] K. M. Ho, C. T. Chan, C. M. Soukoulis, R. Biswas, M. Sigalas, Photonic band gaps in three dimensions: New layer-by-layer periodic structures", *Solid State Commun*., vol. 89 (6), pp. 413-416, 1994.

[25] H. S. Sözüer and J. Dowling, "Photonic Band Calculations for Woodpile Structures", *J. Mod. Opt.*, vol. 41 (2), pp.231-239, 1994.

[26] R. Gonzalo, B. Martinez, C. M. Mann, H. Pellemans, P. H. Bolivar, P. de Maagt, "A low-cost fabrication technique for symmetrical and asymmetrical layer-by-layer photonic crystals at submillimeter-wave frequencies," *IEEE Trans. on Microwave Theory and Techniques*, vol. 50, no.10, pp. 2384-2392, 2002.

[27] I. Ederra, I. Khromova, R. Gonzalo, N. Delhote, D. Baillargeat, A. Murk, B. E. J. Alderman and P. de Maagt "Electromagnetic Band Gap Waveguide for the Millimeter Range", *IEEE Transactions on Microwave Theory and Techniques*, vol. 58 (7), pp. 1734-1741, 2010.

[28] I. Khromova, I. Ederra, R. Gonzalo, and B. P. de Hon, "Symmetrical Pyramidal Horn Antennas Based on EBG Structures", *PIER B*, vol.29, pp. 1-22 (2011).

Irina Khromova was born in Saratov, Russia. She received the M.Phys. degree (with honours) from Saratov State University, Russia, in 2005; the Master degree in communications technology from the Public University of Navarra, Spain, in 2008; the Ph.D. degree in physical and mathematical sciences (with a speciality in laser physics, with honours) from Saratov State University, Russia, in 2008; and a Ph.D. degree in telecommunications engineering (with honours) from the Public University of Navarra, Spain, in 2011.

In 2003, she started working in the Nonlinear Phenomena Group, Saratov State University. In 2005, she joined the Department of Physics, Chair of Laser and Computer Physics, Saratov State University. From 2005 to 2007, she was an Engineer with the Scientific Investigation Department, and a Junior Research Assistant with the Scientific Investigation Department with Saratov State University. Since October 2006, she has been with the Antenna Group, Public University of Navarra. She was a Visiting Researcher with Helhmoltz Institute, Germany (2003), Macquarie University, Australia (2009), the Technical University of Eindhoven, the Netherlands (2010), and Saratov State Technical University, Russia (2011). She has authored 17 articles in peer-reviewed journals and more than 50 conference papers. She is a reviewer in several leading journals on optics, electromagnetism and nonlinear dynamics. Her main fields of scientific interest are electromagnetism, waves and oscillations, fiber and nonlinear optics, plasmonics, microwave and THz physics, laser physics, nonlinear dynamics, and antenna engineering. Her current research concerns electromagnetic waves propagation in electromagnetic band gap structures, photonic crystals, periodic structures with defects, metamaterials, and other types of periodic, anisotropic and nonlinear media; scattering and resonant properties of dielectric, metallic and carbon nanoparticles and their THz applications; and numerical methods for solving electromagnetic problems.

Dr. Irina Khromova is a member of SPIE. She was a recipient of the Dynasty Foundation personal grants for young scientists in 2003, 2004, and 2005. She is a recipient of Laser Optics 2006, Fiber Lasers 2008, 15th Student Seminar on Microwave and Optical Applications of Novel Physical Phenomena, and Metamaterials 2009 best paper awards.

Iñigo Ederra was born in Isaba, Navarra, Spain in 1972. He received the Ingeniero de Telecomunicación and Ph.D. degrees from the Universidad Pública de Navarra, Pamplona, Spain, in 1996 and 2004, respectively.

In 1997, he joined the Microwave and Millimetre Wave Group, Universidad Pública de Navarra. From 1999 to 2000 he was with the European Space Research and Technology Centre (ESTEC), ESA, Noordwijk, The Netherlands, where he was working on Electromagnetic Bandgap materials and their applications in the field of antennas. Since 2001 he is with the Antenna Group, Universidad Pública de Navarra. From June to October 2002 he was visitor scientist at the Rutherford Appleton Laboratory, Chilton, Didcot, UK, participating in the Startiger project. His research interests are in the field of Electromagnetic Bandgap materials and Metamaterials and their applications in microwave, millimetre wave and THz components and antennas.

Dr. Iñigo Ederra was a co-recipient of the LAPC 2006 and IWAT 2007 best paper award.

Jorge Teniente was born in Lodosa, Navarra, Spain in 1973. He received the M.Sc. and Ph.D. degrees from the Public University of Navarra (UPNA), in 1997 and 2003, respectively.

Since 1997, he has been with the Antenna Group of the Public University of Navarra, where he is currently an Associate Professor and has been involved in the research activity of his research group. Between 1999 and 2000, he was a Spanish Trainee at ESA/ESTEC, Noordwijk, The Netherlands. In summer 2002, he was a Research Scientist at the ESA project "StarTiger 1" at Rutherford Appleton Laboratory in England, and from 2004 to 2005, he was at University of Oviedo, Asturias, Spain. Dr. Teniente received the 2nd prize award of the V. Rosina Ribalta in 2003 and the Telefónica Foundation award at the XXIV awards of COIT and AEIT in 2004. His current area of research is in the field of horn antenna technology with emphasis on corrugated horns and space and radio telescope antenna applications. Also, he is involved in terahertz technologies, sub-systems and devices.

Ramón Gonzalo (S'95–M'00) received the M.Sc. degree (with honors) in Telecommunication Engineering in 1995, and the Ph.D. degree in Telecommunication (with honors) from the Universidad Pública de Navarra (UPNa), Spain, in 2000.

Since October 1995, he has been with the Electrical and Electronic Engineering Department, UPNa, where he is Full Professor, acting as Head of Department from March 2008 to December 2010. From September 1997 to December 1998, he was with the Antenna Section, ESA-ESTEC, where he was involved in the modelling and design of EBG antennas at microwave and millimeter-wave frequencies. He has been involved in more than 40 research projects funded by National and International Organisations and Governments. He was acting as Coordinator in more than 20 of them. He has supervised five Ph.D. and more than 25 M. S. dissertations. He has published more than 50 papers in SCI magazines and he has more than 140 conference papers. He has been directly involved in the organisation of three International conferences acting as main organiser and he has been awarded with four prizes to the best paper in different international conferences. His current areas of research are in the field of Metamaterials structures for microwave and millimeter-wave antenna applications with emphasis on space antenna applications and design of imaging systems at submillimeter-wave and THz frequencies.

Karu Esselle (M'92–SM'96) received the B.Sc. degree in electronic and telecommunication engineering (First Class Honors), from the University of Moratuwa, Sri Lanka, and the M.A.Sc. and Ph.D. degrees in electrical engineering from the University of Ottawa, Canada, with a nearly perfect GPA. He is a Professor of electronic engineering at Macquarie University, Sydney, Australia. He was the Immediate Past Associate Dean—Higher Degree Research and the Founding Director of the Postgraduate Research Committee in the Division of Information and Communication Sciences. He held these positions from 2003 to 2008 and was also a member of the Division Executive. He served in all Macquarie University HDR-related committees at the highest level. He is the Director of Electromagnetic and Antenna Engineering, and the Deputy Director of the Research Centre on Microwave and Wireless Applications, which was recently expanded after being recognized as a Concentration of Research Excellence. He has been invited to serve as an international expert/research grant assessor by several overseas nationwide research funding bodies from The Netherlands, Finland, Hong Kong, and Chile. In Australia, he has been invited to assess grant applications submitted to the nation's most prestigious schemes such as Australian Federation Fellowships and Australian Laureate Fellowships. His industry experience includes full-time employment as Design Expert by the Hewlett Packard Laboratory, USA, and several consultancies for local and international companies, including Cisco Systems (USA), Cochlear, Optus Networks, Locata (USA)/QX Corporation, ResMed, FundEd and Katherine-Werke (Germany) through Peter-Maxwell Solicitors.

He was an Assistant Lecturer at the University of Moratuwa, a Canadian Government Laboratory Visiting Postdoctoral Fellow at Health Canada, a Visiting Professor of the University of Victoria and a Visiting Scientist of the CSIRO ICT Centre. He is an Editor of the *International Journal of Antennas and Propagation*. He has authored over 250 scientific publications, including six invited book chapters and over 15 invited conference presentations. His current research interests include metamaterials and their microwave applications, photonic crystals and photonic band gap (PBG)/electromagnetic band gap (EBG) structures, millimeter-wave EBG MMIC devices, antennas based on EBG, periodic structures including frequency selective surfaces, antennas for mobile and wireless communication systems including multi-band WiFi, WiMAX, HyperLAN, and ultra-wideband systems, antennas for multi-signal location and navigation systems, dielectric-resonator (DR) antennas, broadband and multi-band printed antennas, smart antenna systems, hybrid antennas, theoretical methods, lens and focal-plane-array antennas for radio astronomy, moment methods, FDTD methods for periodic structures and closed-form Green's functions for layered structures.

Prof. Esselle's recent awards include the 2009 Vice Chancellor's Award for Excellence in Higher Degree Research Supervision (the first such award ever offered in Macquarie University) and the 2004 (Inaugural) Innovation Award for best invention disclose. Since 2002, he was involved with research grants and contracts worth about five million dollars, and his research team members attracted further grants worth about a million dollars. The CELANE, which he founded, has provided a stimulating research environment for a strong team of researchers including six postdoctoral fellows. His mentees have been awarded six extremely competitive postdoctoral fellowships. Nine international experts who examined the theses of his recent five Ph.D. graduates ranked them in the top 5% or 10% in the world. He has served on technical program committees or international committees for many international conferences. He will be chairing the Technical Program Committee of APMC 2011; he was the Publicity Chair of the APMC 2000. He is the Chair of the IEEE New South Wales (NSW) MTT/AP Joint Chapter, an Editor of the Macquarie University Engineering Colloquia (MQEC), the past Chair of the Educational Committee of the IEEE NSW, and a member of the IEEE NSW Committee.